Equivalent Contact Length of Load Disks and Specimen

Jiří Ondrášek(✉)

1VÚTS, a.s., Liberec, Czech Republic
jiri.ondrasek@vuts.cz

Abstract. The paper deals with a method of performing experimental tests to test the service life of a general kinematic pair of cam mechanisms with a roller follower. In the case of the test rig, the general kinematic pair is formed by the contact surface of a cylindrical specimen in contact with three load disks. The specimen represents the loaded cam and the disks a roller follower. The disk profile shape has a significant effect on the stress distribution in the surface layers of specimens due to their load. The disk profile is expressed by an equivalent width, which is determined by the finite element method.

Keywords: Cam mechanism · General kinematic pair · Test rig · Contact stress · Disk shape · Equivalent contact length

1 Introduction

Conventional cam mechanisms are characterized by the ability to transfer high powers at high speed and positional accuracy; their applicability is mainly connected with the so-called hard automation that is characterized by unchangeable or difficult to change actions of the given technical equipment. A cam mechanism is a three-link mechanical system with one degree of freedom that contains at least one cam connected to the other links by at least one general kinematic pair (GKP). Through the working surface of the cam (driving link), the motion of the driven link via GKP is derived. The driven link is called a follower. The follower performs a translating, oscillating or general motion. The general kinematic pair is formed by the contact of the cam and the follower.

The force ratios in the general kinematic pair formed by the contact of the cam and the follower cause the contact stresses. The main stresses that have the character of pulses with a period of 2π depending on the cam angular displacement ψ characterize the state of the stress on the cam working surface and thereunder. These are transient compressive stresses. In the surface layers of the material stressed in this way, variable elastic or elastoplastic strains occur. Exceeding a certain limit of these stresses can cause fatigue damage of the working surfaces of the cam and the follower after a certain number of cycles of the cam mechanism operation. This damage (pitting) results in the form of pits that develop from the cracks on the working surface.

In general, the fatigue is caused by progressive and localized structural damage which occurs in the material under cyclic loading. The maximum load stress values σ_{red} do not

J. Beran et al. (Eds.): TMM 2020, MMS 85, pp. 62–69, 2022.
https://doi.org/10.1007/978-3-030-83594-1_7

reach the ultimate tensile strength σ_U and may be below the tensile yield strength σ_Y of the material. The maximum load stress values have to be limited by the tension-loaded material fatigue strength σ_C. The fact that during the operation of the cam mechanisms, no destructive action of elastic deformation occurs in the general kinematic pair, it is described by the conditional inequality [1]

$$\max(\sigma_{red}(\psi, z)) < \sigma_Y, \psi \in \langle 0, 2\pi), z \geq 0 \tag{1}$$

where variable z expresses the depth under the loaded surface. The conditional inequality Eq. (1) is valid for steel materials. Thus, the mechanical properties of the material of a cam or follower working surface have a significant effect on the occurrence of fatigue damage. Equally important is the information describing the heat or chemical-heat treatment and its effect on the properties of the internal structure of the material. The material of bodies in contact must be of high quality, any imperfection or inclusion acts as a crack initiation site. The surface of the material should be as smooth as possible, without unevenness, to prevent the propagation of cracks from the body surface. Lubrication has a significant effect on the contact fatigue as well.

2 Experimental Method

The aim of the experiments is to achieve the fatigue damage of the specimen contact surface after a certain number of cycles depending on the magnitude of the loading force, specimen material, lubrication of contact surfaces, type of lubricant used, type of coatings being applied to the specimen contact surface, disk crown profile etc. Experiments can take place: when the contact surfaces are mutually rolling or at a certain value of the slippage of the contact surfaces. In this way, we can obtain complete lifetime curves for a certain material with specific properties and then we can use them in designing other cam mechanisms.

2.1 Test Rig

Testing can be carried out on a device which allows a simulation of the state on a radial cam or an axial cam with a roller follower. As shown in Fig. 1, the cylindrical test specimen 5 of a defined width is placed on the shaft between three disks, one of which is a pressure disk 4 and the other two are fixed (2 and 3). The disks are arranged on a common plane at the vertices of an equilateral triangle with the length of its sides s. The axes of rotation of the disks are parallel. Pressure disk 4 is rotationally mounted on one of the arms of the pivotally mounted two-arm lever 6 with the arm length l. The two-arm lever is coupled through the other arm to the application place of the pressing force N of a defined magnitude. In terms of the geometric arrangement of the loading disks and the loaded specimen, the specimen is loaded by three equal reactions N, individually from each disk. Due to the rotation of the tested body 5 between three disks rotating with the same angular velocity Ω_2, the pressing force N has the character of pulses with the period of $2\pi/3$. It is therefore a transient loading. Due to the contact at three locations, the testing time is reduced to 1/3, which greatly simplifies testing as each specimen is tested for 10^7 to 10^8 cycles. In analogy with the cam mechanism with a cam and a roller

follower, loading bodies 2, 3 and 4 represent a cylindrical roller and the loaded body 5 corresponds to the cam.

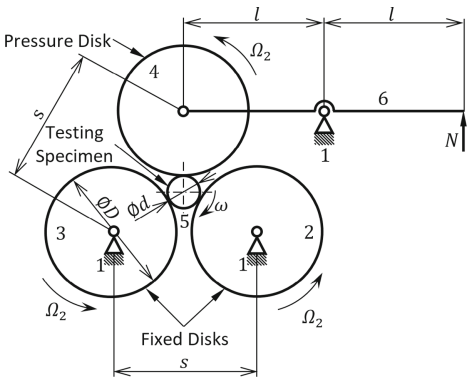

Fig. 1. Kinematic scheme of the conceptual design of a test rig.

2.2 Shape of Surfaces in Contact

When examining the factors that influence the contact fatigue, it was published [2] that the shape of the surfaces in contact has a significant effect. Due to the nature of the course of tests, it is advisable that the contact stress is distributed as evenly as possible for various load levels.

The disk profile has a significant effect on the stress distribution due to the load in the surface layers of specimens. In the case of a conventional cylindrical profile of the disks, there are discontinuities at the intersections of their cylindrical profile with the cylindrical profile of the specimen, i.e. if one contact part is axially shorter than the other, and also when the edges of the disks are chamfered, see Fig. 2. The mentioned discontinuities cause a very sharp increase in pressure distribution in the respective contact area of the bodies. These local increases in the pressure distribution can exceed the ultimate strength of the given material and thus cause plastic deformations, residual stresses in the material or change in the steel structure. Furthermore, the region concerned will be more prone to fatigue damage of the contact surfaces, i.e. to pitting or spalling. In the case of the cylindrical disk, the contact between the disk and the specimen cannot be considered as simply straight, but as a more complex three-dimensional type of contact.

The excessive edge stress in the case of the cylindrical disks can be reduced via such a shape of the axial cross-section of the disk crown that includes a straight line and one circular arc or a combination of several circular arcs, see Fig. 2. Such a shape of the disk crown one segment of which is cylindrical and the adjoining one is convex, causes a certain stress concentration during the transfer from the cylindrical region to the convex one. The radius of curvature ρ_y characterizes the convex segments in the plane Oyz. The size of the radius of curvature ρ_y is the subject of optimization of the disk profile in order that the distribution of the contact stress generated by the effects of the force N was as evenly as possible. This disk type was chosen for the test rig because of the acceptable technological complexity of its manufacturing in desired quality and accuracy.

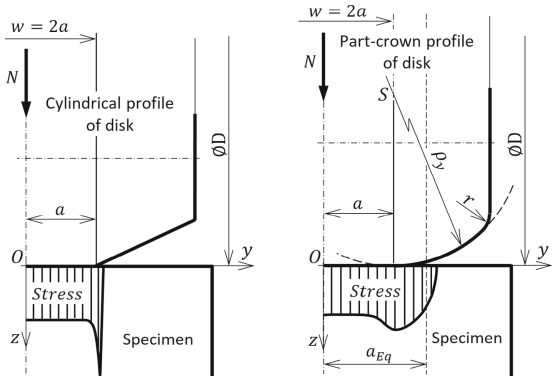

Fig. 2. Schematic drawing of the disk profiles.

2.3 Contact of Two Cylindrical Bodies

In order to calculate the contact stresses distribution in the contact regions of the load disks and the specimen, it is possible to use both the results of the contact mechanics [3] for the respective case of the contact of two elastic bodies and the finite element method [4, 5]. Hertzian contact stress theory [3] is applied to the contact of cylindrical bodies with parallel axes, see Fig. 3. Using this theory, it is possible to calculate the strain and stress components in both bodies in the contact surface and its vicinity.

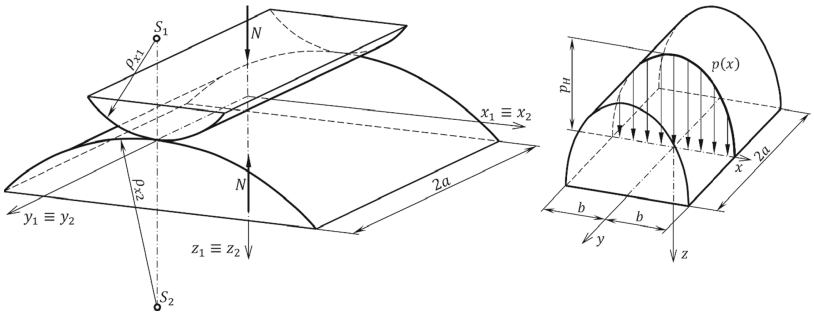

Fig. 3. Contact of two cylindrical bodies.

When two cylindrical bodies are brought into contact, they touch initially along a line. Under the action of a slightest load N, they will deform and contact is made over a finite area of length $2a$ and width $2b$ which is relatively small, compared with the dimensions of both bodies. The coordinate system $Oxyz$ is located in its center. The contact pressure $p(x)$ is distributed according to the elliptical cylinder and its maximum value is called Hertzian pressure, which is derived based on Hertzian contact theory [3]

$$p_H = \sqrt{\frac{NE^*}{\pi 2aR_e}}, \frac{1}{E^*} = \frac{1-\nu_1^2}{E_1} + \frac{1-\nu_2^2}{E_2}, \frac{1}{R_e} = \frac{\text{sign}(\rho_{x2})}{\rho_{x1}} + \frac{1}{|\rho_{x2}|} = \frac{2(D+d)}{Dd} \quad (2)$$

E^* is the effective modulus of elasticity, E_i and ν_i are the respective Young's modulus of elasticity and Poisson's ratio of the individual solids. The geometry of the two contacting cylinders is described with the equivalent radius of curvature R_e where $\rho_{x1} = D/2$ denotes the radius of the loading disks and $\rho_{x2} = d/2$ is the radius of the specimen. The half-width b of the contact area is determined as [3]

$$b^2 = 4f\, R_e \big/ \left(\pi\, E^*\right),\ f = N \big/ (2a) \tag{3}$$

The contact stress state existing on the symmetry plane yz is determined by the actual main stress components $\sigma_x, \sigma_y, \sigma_z$. These quantities are assumed as compressive stresses and their absolute value decreases in proportion to a distance z from the contact area. The stress components are given by the expressions [3]

$$\sigma_x = -p_H \left(\frac{1+2\xi}{\sqrt{1+\xi^2}} - 2\xi \right), \sigma_y = -2\nu p_H \left(\sqrt{1+\xi^2} - \xi \right), \sigma_z = -p_H \frac{1}{\sqrt{1+\xi^2}} \tag{4}$$

where the proportional independent variable $\xi = z \big/ b$ is introduced. The stress distribution in the planar interface is given by the relations [3]

$$\sigma_x = \sigma_z = -p_H \sqrt{1 - \left(x \big/ b\right)^2},\ \sigma_y = -2\nu p_H \sqrt{1 - \left(x \big/ b\right)^2} \tag{5}$$

The Tresca yield criterion can be used to find the reduced stress σ_{red}, according to which this theory can be considered in terms of the maximum sliding stress, proportional to the difference of the main stresses [6]

$$\sigma_{red} = \max\left\{ \left|\sigma_x - \sigma_y\right|,\ \left|\sigma_z - \sigma_x\right|,\ \left|\sigma_z - \sigma_y\right| \right\}, \max(\sigma_{red}) = 0.6 p_H \tag{6}$$

When the cylindrical bodies come into contact, the largest value of the reduced stress $\max(\sigma_{red})$ is at a given depth z_e below the surface and reaches the size according to Eq. (6) [1]. Based on Eqs. (1), (2) and (6), we can formulate a condition for determining the limit value of the amplitude of the loading force N so that plastic deformations will not occur under the contact surface during the operation

$$N \le \frac{\pi 2 a R_e}{E^*} \left(\frac{K_R \sigma_U}{0.6} \right)^2, K_R = \frac{\sigma_Y}{\sigma_U} \in \langle 0.55,\ 0.8 \rangle \tag{7}$$

Constant K_R expresses the ratio of the yield tensile strength $\sigma_Y R_{p0.2}$ just to the ultimate strength σ_U.

2.4 Equivalent Contact Length of Load Disks and Specimen

In order to determine the shape of the contact area of the load disks and the specimen, the components of strains and stresses in both bodies around the contact area, it is necessary due to the above given shape of the disks profile to determine equivalent contact length $2a_{Eq}$ in contact of the load disks with the specimen. This equivalent

length $2a_{Eq}$ will be greater than the width w of the cylindrical part of the disk $2a_{Eq} > w$ and will depend on the size of the loading force N. In accordance with [4, 5], FEM models of the disk and specimen contact have been created for a set of loading forces $N = \{0.25,0.50,1,2,3,4,6,8,10\}\cdot 10^3 N$ and $w = 3$ mm. By analyzing the results of the distribution of the contact stress and the contact pressure listed in Table 1, we determined the computational relation for the estimation of the equivalent length $2a_{Eq}$ of the contact surface in the contact of the load disks and the specimen

$$N(w = 3\,\text{mm}) = 3532.7\left(2a_{Eq}\right)^3 - 36235\left(2a_{Eq}\right)^2 + 124108\left(2a_{Eq}\right) - 141594 \quad (8)$$

assuming that both parts are made of steel. In Table 1, the variables $\bar{\sigma}_{red}$ and $\bar{p}_H$ represent respectively the mean value from the course of the largest values of the reduced contact stress $\max(\sigma_{red})$ in the plane of symmetry Oxz and from the course of the values of the Hertz pressure p_{H} on the contact surface Oxy. From Eq. (8), e.g. by Newton's numerical method, we can determine the appropriate length $2a_{Eq}$ for a given load N and a set of load disks. Examples of the distribution of the reduced stress in the plane of symmetry Oxz and the contact pressure in the contact plane Oxy are shown in Fig. 4 to Fig. 7.

Table 1. Contact stress for the width of the cylindrical part of the disk $w = 3$ mm.

N [N]	$\bar{\sigma}_{red}$ [MPa]	$\bar{p}_H$ [MPa]	$2a_{Eq}$ [mm]
250	320.00	570.00	3.22
500	430.00	780.00	3.73
1000	600.00	1050.00	3.95
2000	800.00	1400.00	4.17
3000	950.00	1700.00	4.30
4000	1100.00	1950.00	4.41
6000	1300.00	2300.00	4.57
8000	1500.00	2600.00	4.70
10000	1650.00	2900.00	4.80

We can then use the values of the variable a_{Eq} in the relations for the calculation of the main stresses, the geometry of the two contacting cylinders, the contact pressure and the limit value of the amplitude of the loading force N according to the Eqs. (2), (3), (4) and (7).

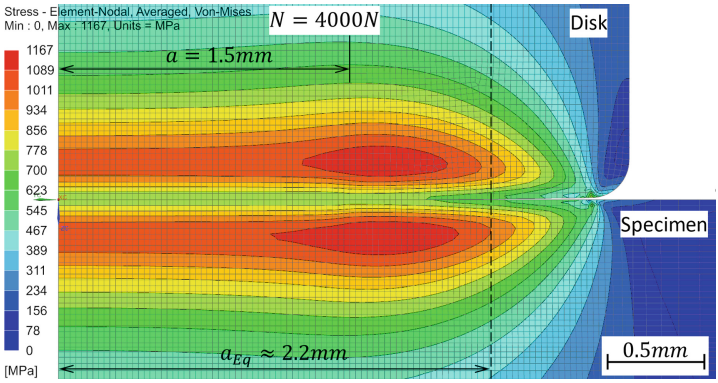

Fig. 4. Reduced stress.

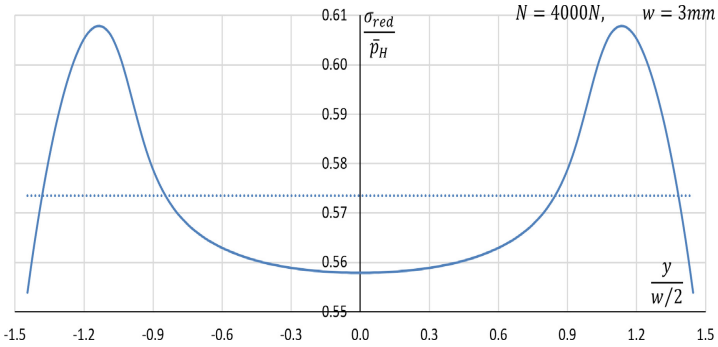

Fig. 5. Relative expression of reduced stress.

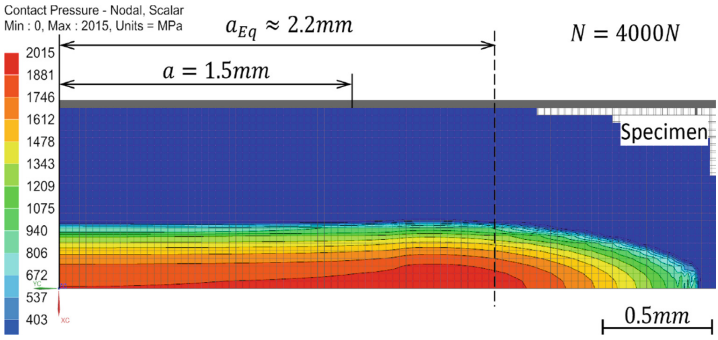

Fig. 6. Contact pressure.

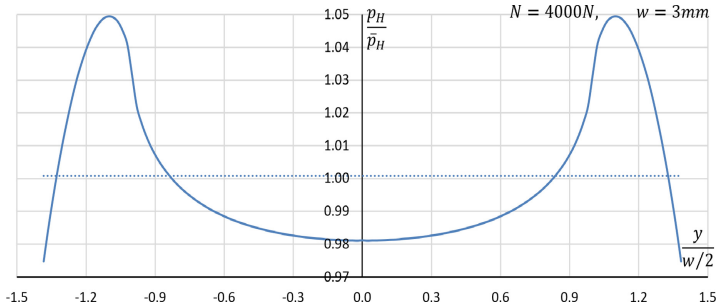

Fig. 7. Relative expression of contact pressure.

3 Conclusion

The paper presents a method for evaluating the contact stress of a cylindrical sample, which is loaded in a test device with three rotating disks. In order to distribute the contact stress as evenly as possible, the loading disks are provided with a part-crown shape of the profile. In analogy with a cam mechanism with a roller follower, the loaded specimen corresponds to the cam and the loading disks represent a cylindrical roller. In this case, the disk profile is expressed by an equivalent width, which is determined based on the finite element method. We can then use the value of the equivalent width in the formulas to evaluate the components of the contact stresses and the strains of cylindrical bodies with the parallel axes according to the methods of contact mechanics.

References

1. Koloc, Z., Václavík, M.: Cam mechanisms, 1st edn. Elsevier, Amsterdam (1993)
2. Norton, R.L.: Cam design and manufacturing handbook. 2nd ed. Industrial Press, Inc., New York (2009). ISBN 978–0–8311–3367–2.
3. Johnson, K., L.: Contact mechanics. 1st edn. Cambridge University Press, Cambridge (1985). ISBN 0 521 34796 3.
4. Ondrášek, J.: Effect of the roller crown shape on the cam stress. In: Corves, B., Wenger, P., Hüsing, M. (eds.) EuCoMeS 2018. MMS, vol. 59, pp. 223–230. Springer, Cham (2019). https://doi.org/10.1007/978-3-319-98020-1_26
5. Jiří, O. The general kinematic pair of a cam mechanism. In: Joseph, M. (ed.) Kinematics - analysis and applications, IntechOpen, (2019). https://doi.org/10.5772/intechopen.86682. https://www.intechopen.com/books/kinematics-analysis-and-applications/the-general-kinematic-pair-of-a-cam-mechanism.
6. Vable, M.: Mechanics of materials, 2nd ed., Section 10.3, Failure theories, pp. 486–492, MTU. http://www.me.mtu.edu/~mavable/MoM2nd.html.